

Automated Indexing for Texture and Strain Measurement with Broad-Bandpass X-ray Microbeams

Jin-Seok Chung and Gene E. Ice

*Metals and Ceramics Division
Oak Ridge National Laboratory 37831-6118*

Abstract

Methods are derived for measuring local strain, stress, and crystallographic texture (orientation) in polycrystalline samples when 1-10 grains are simultaneously illuminated by an energy scanable or broad-bandpass x-ray beam. The orientation and unit cell shape for each illuminated grain can be determined from the diffracted directions of four Bragg reflections. The unit cell volume is determined by measuring the energy (wavelength) of one reflection. The methods derived include an algorithm for simultaneously indexing the reflections from overlapping crystal Laue patterns and for determining the average strain and stress tensor of each grain. This approach allows measurements of the local strain and stress tensors which are impractical with traditional techniques.

Introduction

The development of ultra-brilliant 3rd-generation synchrotron x-ray sources^{1,2} together with recent advances in x-ray optics^{3,4} has created intense x-ray microbeams which can be used to study materials properties with submicron spatial resolution. X-ray microdiffraction is a particularly promising tool for the study of strain and texture distributions. However, traditional measurement techniques are unsuitable for x-ray microdiffraction; too few grains are illuminated for powder diffraction and monochromatic single-crystal techniques cannot be used because the sample volume changes when the sample is rotated (Fig. 1).

White-beam Laue diffraction is a standard crystallographic method used to determine crystal orientation without rotation of the sample.^{5,6} However, Laue diffraction is rarely used to measure strain because the precision of most Laue instruments is low compared to modern diffractometers, and because the unit cell volume cannot be determined with a standard Laue measurement. Nevertheless, with suitable instrumentation, the Laue method can be used to precisely determine the orientation (local texture) of individual grains and their

distortion strain. Laue diffraction can also be extended by measuring the energy of one or more reflections to determine the full strain tensor in polycrystalline samples.

In order to measure strain *distributions*, a large number of measurements must be collected. This process requires automated methods such as the ones outlined below. Of course these methods can also be applied to studies with larger beams using standard x-ray sources.

The actual process of measuring strain in polycrystalline samples with microprobe beams is outlined in Fig. 2 below. A broad-bandpass microbeam intercepts a sample and illuminates a small number of crystal grains. The overlapping Laue patterns from the grains are recorded on an area detector and fit to find the center of each reflection. The pattern is then indexed to determine the indices of each reflection and the number of reflecting grains. Finally, the texture (orientation) and relative or absolute strain tensors are determined for the illuminated grains.

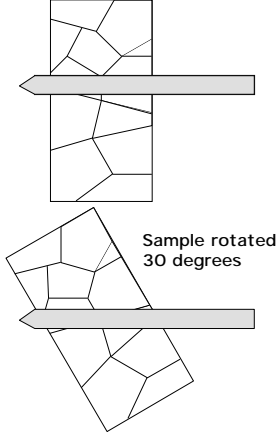


Fig. 1 A small penetrating x-ray beam intercepts various grains in a polycrystalline sample which change as the sample is rotated. Different grains are illuminated because (a) the penetrating beam has a high depth to transverse cross-section ratio, which in polycrystalline samples makes it impossible to ensure that the same grains are illuminated as the sample is rotated, and (b) because the sphere of confusion for state-of-the-art diffractometers is greater than $1\mu\text{m}^3$.

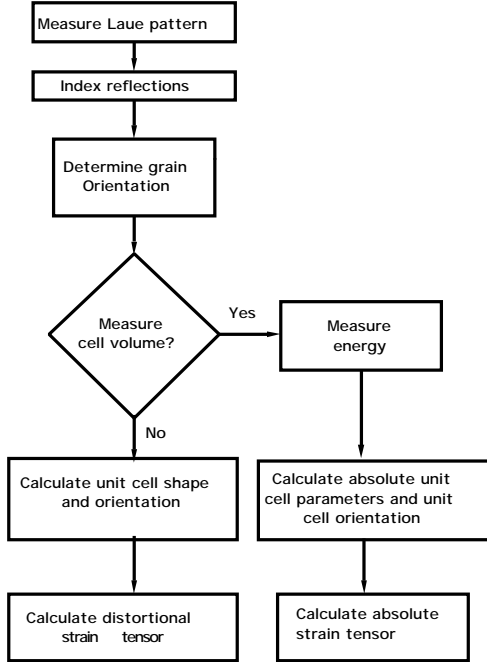


Fig. 2 Flow chart for calculating the strain in a polycrystalline sample using an x-ray microbeam.

The organization of this paper traces backward through the flow chart of Fig. 2. We first demonstrate how the strain tensor is determined by the unit cell, then show how the unit cell parameters are determined, and finally show how the reflections are automatically indexed.

The key step in this process is indexing the Laue spots. The indexing approach outlined in this paper is quite distinct from methods which have been described previously^{7,8,9}, and has the advantages that it requires only a few reflections (>4 per grain), and can process overlapping Laue patterns generated by multiple grains.

Strain from unit cell parameters

Single crystal diffraction directly measures the average local strain tensor of the crystal through the orientation of the unit cell and the distortion of the lattice parameters from their (unstrained) values. Consider for example a unit cell with lattice parameters a_i and α_i and a Cartesian coordinate system \mathbf{u}_i which is attached to the crystal. We adopt a notation where the vector \mathbf{a}_1 is coincident with the \mathbf{u}_1 axis, \mathbf{a}_2 is in the $\mathbf{u}_1\mathbf{u}_2$ plane, and \mathbf{u}_3 is perpendicular to the $\mathbf{u}_1\mathbf{u}_2$ plane (see Fig. 3). Similar notations have been adopted by previous authors.^{10,11,12}

A position in the crystal can be specified either by a vector in the Cartesian coordinates \mathbf{v}_u or by a vector with unit cell coordinates \mathbf{v} . The transformation from unit cell coordinates to Cartesian coordinates is given by

$$\mathbf{v}_u = \mathbf{A}\mathbf{v}$$

where

$$\mathbf{A} = \begin{pmatrix} a_1 & a_2 \cos \alpha_3 & a_3 \cos \alpha_2 \\ 0 & a_2 \sin \alpha_3 & -a_3 \sin \alpha_2 \cos \beta_1 \\ 0 & 0 & 1/b_3 \end{pmatrix}.$$

(1)

Here the β_s s and b_s s are the reciprocal lattice parameters for the unit cell.

A vector position attached to a crystal can move due to rigid body translation of the crystal, due to rigid body rotation of the crystal, or due to distortion of the crystal lattice (strain).¹³ The average strain of a measured unit cell can be determined by comparing the measured unit cell parameters to the unit cell parameters of undistorted material. Let \mathbf{A}_{Meas} be the matrix which converts a measured vector \mathbf{v} into the measured crystal Cartesian coordinates. Let \mathbf{A}_0 be the matrix for an *unstrained* unit cell which converts \mathbf{v} into the Cartesian reference frame of the measured (strained) crystal. To ensure that there is no rigid body translation between the measured unit cell and the unstrained unit cell, the origin of the unit cell vectors are made coincident. For convenience, we assume \mathbf{a}_1 of the unstrained unit cell lies along the \mathbf{u}_1 axis and \mathbf{a}_2 of the unstrained unit cell to lie in the $\mathbf{u}_1\mathbf{u}_2$ plane.

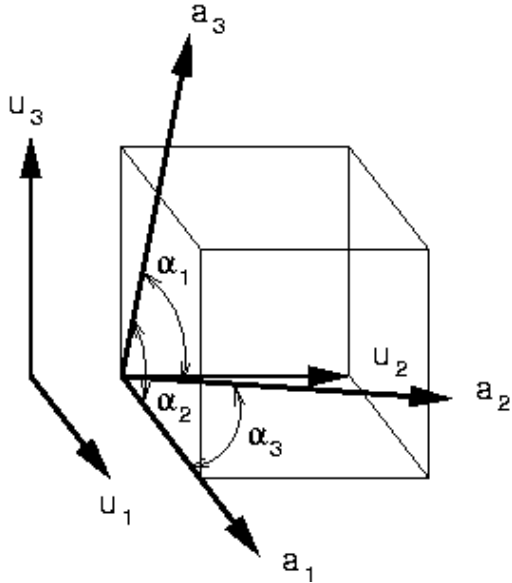


Fig. 3 Cartesian coordinates attached to the real-space unit cell. Note that $\mathbf{u}_1 = \mathbf{a}_1 / |\mathbf{a}_1|$; $\mathbf{u}_3 = \mathbf{a}_1 \times \mathbf{a}_2 / |\mathbf{a}_1| |\mathbf{a}_2| \sin \alpha$; and $\mathbf{u}_2 = \mathbf{a}_3 \times \mathbf{a}_1$.

A position vector \mathbf{v} in the unit cell coordinates is found in the measured-crystal Cartesian coordinate reference frame at

position $\mathbf{A}_0 \mathbf{v}$ for the unstrained case and at position $\mathbf{A}_{\text{Meas}} \mathbf{v}$ for the strained case. With this definition, for the matrices \mathbf{A}_{Meas} and \mathbf{A}_0 there is a transformation matrix \mathbf{T} which maps from unstrained to strained vectors.

$$\mathbf{A}_{\text{Meas}} = \mathbf{T} \mathbf{A}_0 \quad (2)$$

The transformation matrix can include both distortion and rotation terms and for unstrained crystals $\mathbf{T} = \mathbf{I}$. From the definition of the strain tensor, ϵ_{ij} , the strain tensor in the measured-crystal Cartesian-coordinate reference frame is given by,

$$\epsilon_{ij} = (\mathbf{T}_{ij} + \mathbf{T}_{ji}) / 2 - \mathbf{I}_{ij}. \quad (3)$$

The strain tensor in the crystal reference frame can be converted to a laboratory reference frame or to a sample reference frame by using a rotation matrix \mathbf{R} .

$$\epsilon_{ij}^{\text{Sample}} = \mathbf{R} \epsilon_{ij} \mathbf{R}^{-1} \quad (4)$$

The strain tensor of Eq. 3 contains both a hydrostatic strain (dilatation) and a distortion strain term. With the hydrostatic strain, $\Delta/3$ defined as the mean strain component along each Cartesian axis, Eq. 3 can be written in terms of the two components,

$$\epsilon_{ij} = \begin{pmatrix} \epsilon_{11} - \frac{\Delta}{3} & \epsilon_{12} & \epsilon_{13} \\ \epsilon_{12} & \epsilon_{22} - \frac{\Delta}{3} & \epsilon_{23} \\ \epsilon_{13} & \epsilon_{23} & \epsilon_{33} - \frac{\Delta}{3} \end{pmatrix} + \begin{pmatrix} \frac{\Delta}{3} & 0 & 0 \\ 0 & \frac{\Delta}{3} & 0 \\ 0 & 0 & \frac{\Delta}{3} \end{pmatrix} \quad (5)$$

where $\Delta = \epsilon_{11} + \epsilon_{22} + \epsilon_{33}$

Here the first term is the distortion term and the second term is the dilatation term. With microdiffraction measurements, it is important to retain the full (9 parameter) information contained in the crystal strain tensor *and* local grain orientation; the stress tensor can be determined from the strain tensor and the anisotropic single crystal elastic constants (stiffness moduli).¹³

$$\sigma_{ij} = \sum_{kl} C_{ijkl} \epsilon_{kl} \quad (6)$$

Orientation and unit cell constants from monochromatic reflections

With monochromatic diffraction, it is well known, that two non-colinear reflections are required to determine the orientation of a crystal.¹⁰ Three independent reflections determine the orientation *and* unit cell parameters of an unknown (i.e. strained) crystal.¹⁰

With a wide-bandpass (or tunable) beam, the Bragg condition can be met for more than one reflection, without rotating the sample. However, the energy of each reflection must be measured to determine the diffraction vector. For example, if the energy of the incident beam is scanned while an area detector is monitored for Bragg reflections, the angles and energies of \mathbf{n} reflections can be collected. The problem of determining the unit cell parameters and crystal orientation with this method is virtually identical to monochromatic beam measurements and again two independent reflections determine the orientation of a known unit cell while three independent reflections determine the orientation *and* unit cell parameters of an unknown unit cell.

Although measurements with a scanable beam have very definite advantages (low thermal load, reduced number of reflections needed, etc.), the method is inherently slow compared to measurements with broad-bandpass or white beams which simultaneously meet the Bragg condition for several reflections (Fig. 4).

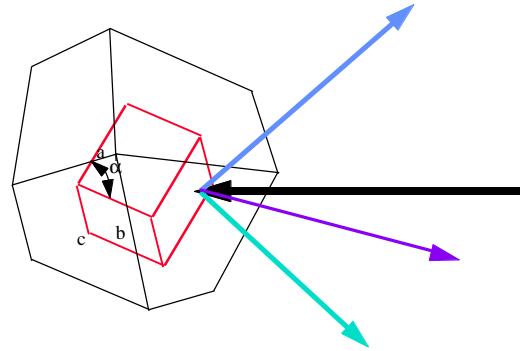


Fig. 4 Broad-bandpass radiation can simultaneously excite several reflections.

Determination of crystal orientation from two white-beam reflections

With white-beam Laue diffraction, the volume of a unit cell (dilatation) cannot be unambiguously determined. For example, as shown in Fig 5, two unit cells with the same relative shape and orientation create identical Laue patterns although they have very different volumes. The *energies* of the reflections are, however, sensitive to the d spacing and hence to the volume of the unit cell. We show later that the volume of the unit cell can be determined by measuring the energy of *one* of four independent reflections or by measuring the energies of three independent reflections.

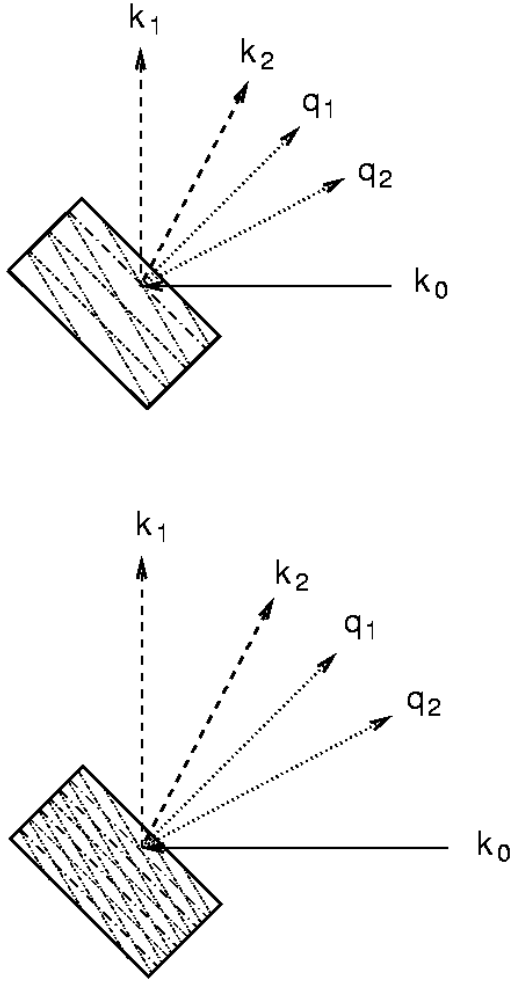


Fig. 5 For two unit cells with the same relative shapes and orientations, the Laue patterns will look the same. However, the energies of the reflections depend on the d spacing and hence the volume of the unit cell.

As described by Busing and Levy¹⁰, it is convenient to work in reciprocal lattice space to calculate crystal plane normals. We adopt an approach similar to that of Busing and Levy¹⁰ with a second Cartesian coordinate system attached to the crystal. The x axis is parallel to the crystal reciprocal axis \mathbf{b}_1 , the y axis is in the plane of \mathbf{b}_1 and \mathbf{b}_2 , and the z axis is perpendicular to the $\mathbf{b}_1\mathbf{b}_2$ plane. With this definition, a vector \mathbf{v}_R can

be transformed from reciprocal-lattice coordinates to the xyz reciprocal-lattice Cartesian-coordinates with the transformation,

$$\mathbf{v}_c = \mathbf{B}\mathbf{v}_R \quad (7)$$

where,

$$\mathbf{B} = \begin{pmatrix} b_1 & b_2 \cos \beta_3 & b_3 \cos \beta_2 \\ 0 & b_2 \sin \beta_3 & -b_3 \sin \beta_2 \cos \alpha_1 \\ 0 & 0 & 1/a_3 \end{pmatrix} \quad (8)$$

Here again, the a_i 's and α_i 's the b_i 's and β_i 's are the real-space and reciprocal lattice parameters respectively. Vectors in the reciprocal-lattice Cartesian coordinate system can be further transformed into a laboratory Cartesian coordinate system if the orientation of the crystal is specified through an orientation matrix \mathbf{U} such that

$$\mathbf{v}_{\text{Lab}} = \mathbf{U}\mathbf{v}_c \quad (9)$$

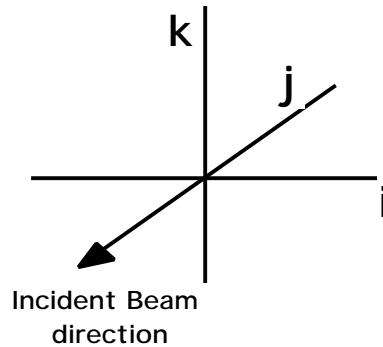


Fig. 6 The reciprocal-lattice crystal-coordinate system xyz is coincident with the laboratory ijk reference frame when $\mathbf{U}=\mathbf{I}$. Note that incident beam has a $-\mathbf{j}$ direction.

With this definition, the normal of a reflection h,k,l in the laboratory Cartesian co-ordinate system is given by,

$$\mathbf{n}_{hkl} = \frac{\mathbf{UB} \begin{pmatrix} h \\ k \\ l \end{pmatrix}}{\left| \mathbf{UB} \begin{pmatrix} h \\ k \\ l \end{pmatrix} \right|}. \quad (10)$$

Experimental measurements consist of beam intercepts on a detector referenced to the laboratory reference frame \mathbf{r}_{hkl} . If the energy of the x-ray beam is unknown, then the direction of the reflection (normal of the Bragg planes) is determined but the magnitude of the momentum transfer \mathbf{h} is not determined. The normal to the Bragg plane is given by,

$$\mathbf{n}_{hkl}^M = \frac{\hat{\mathbf{r}}_{hkl} + \mathbf{j}}{|\hat{\mathbf{r}}_{hkl} + \mathbf{j}|}. \quad (11)$$

Assume that there are two observed reflections with known indices, denoted as the **primary** and **secondary** orienting reflections. From the experimental observations, we know the plane normals for the two reflections in the laboratory reference frame \mathbf{n}_{M1} , \mathbf{n}_{M2} . Since the indices and unit-cell parameters, \mathbf{B} , are known, we can calculate the Bragg plane normals in the laboratory reference frame if the orientation matrix \mathbf{U} is known:

$$\mathbf{n}_{M1} = \mathbf{UB} \begin{pmatrix} h \\ k \\ l \end{pmatrix}_1 \quad (12)$$

The ideal orientation matrix \mathbf{U} satisfies Eq. 12 for both the primary and secondary orienting reflections. However, as described

by Busing and Levy¹⁰, due to experimental errors or lattice strain, it is not in general possible to find an orthogonal matrix \mathbf{U} that simultaneously satisfies both conditions. Indeed there are four independent equations which must be satisfied by only three rotations parameters. The standard practice is, therefore, to insist that the primary reflection satisfies Eq. 12 and to further constrain \mathbf{U} so the secondary reflection calculated from Eq. 10 lies in the plane which contains the experimental normals.¹⁰

Orientation and distortion strain from four white-beam reflections

When the unit-cell parameters are unknown (i.e., strained crystal), it is still possible to determine the orientation and *distortion strain* of the unit cell if four independent broad-bandpass reflections are observed. Here we seek to find matrices \mathbf{U} and \mathbf{B} that simultaneously satisfy four observed normal directions. Each normal has two direction angles, so with four independent normals, there are a total of eight independent equations to solve for the 9 unknowns (3 crystal rotations, 6 unit cell parameters). However, since the dilatation term cannot be determined without an energy measurement (Fig. 5), we restrict ourselves to the determination of the orientation and distortion strain.

From Eq. 5, the diagonal elements of the distortion strain tensor must sum to zero, hence the distortion-strain tensor can be written with 5 unknowns, where the $\epsilon_{ii}^* = \epsilon_{ii} - \Delta/3$.

$$\epsilon_{ij}^\delta = \begin{pmatrix} \epsilon_{11}^* & \epsilon_{12} & \epsilon_{13} \\ \epsilon_{12} & \epsilon_{22}^* & \epsilon_{23} \\ \epsilon_{13} & \epsilon_{23} & -\epsilon_{11}^* - \epsilon_{22}^* \end{pmatrix} \quad (13)$$

If dilatation is ignored, there are, therefore, a total of 8 unknowns about the crystal orientation and the unit cell parameters.

Suppose the normal directions \mathbf{n}_i of four reflections \mathbf{h}_i are measured. In order to determine distortion and orientation, each of the four subsets of three reflections must be linearly independent. The momentum transfer vectors are then related to the normals and to each other through scale factors s_i which we define as,

$$\begin{aligned}\mathbf{h}_1 &= s_1 s_3 \mathbf{n}_1 \\ \mathbf{h}_2 &= s_2 s_3 \mathbf{n}_2 \\ \mathbf{h}_3 &= s_3 \mathbf{n}_3 \\ \mathbf{h}_4 &= c_1 \mathbf{h}_1 + c_2 \mathbf{h}_2 + c_3 \mathbf{h}_3 .\end{aligned}\quad (14)$$

Here, the c_i are determined by the reflection indices, and s_3 is an overall unit cell scale factor which cannot be determined without energy measurements. To find s_1 and s_2 , we use,

$$\frac{\mathbf{j} \cdot \mathbf{n}_4}{\mathbf{k} \cdot \mathbf{n}_4} = \frac{(c_1 s_1 \mathbf{n}_1 + c_2 s_2 \mathbf{n}_2 + c_3 \mathbf{n}_3) \cdot \mathbf{j}}{(c_1 s_1 \mathbf{n}_1 + c_2 s_2 \mathbf{n}_2 + c_3 \mathbf{n}_3) \cdot \mathbf{k}}$$

and

$$\frac{\mathbf{i} \cdot \mathbf{n}_4}{\mathbf{k} \cdot \mathbf{n}_4} = \frac{(c_1 s_1 \mathbf{n}_1 + c_2 s_2 \mathbf{n}_2 + c_3 \mathbf{n}_3) \cdot \mathbf{i}}{(c_1 s_1 \mathbf{n}_1 + c_2 s_2 \mathbf{n}_2 + c_3 \mathbf{n}_3) \cdot \mathbf{k}}\quad (15)$$

The two equations above are used to solve for the two unknown ratios $s_1 = |\mathbf{h}_1|/|\mathbf{h}_3|$ and $s_2 = |\mathbf{h}_2|/|\mathbf{h}_3|$.

Once s_1 and s_2 are known, the direction normals and relative magnitudes of any reciprocal-lattice reflections can be determined in the laboratory reference frame (eg. $|\mathbf{b}_1/\mathbf{b}_3|$, $|\mathbf{b}_2/\mathbf{b}_3|$, \mathbf{n}_{100} , \mathbf{n}_{010} , \mathbf{n}_{001}). From the definitions which led to equation 8, and assuming that the product $b_{11}b_{22}b_{33}$ is known from the unstrained unit cell (no dilatation), the reciprocal-lattice Cartesian coordinates can then be specified and, therefore, the matrices \mathbf{B} and \mathbf{U} .

Full strain tensor

Once the unit cell shape and orientation have been determined, the volume can be

unambiguously determined by measurement of the energy of a single reflection. This gives the lattice spacing of the reflection and, therefore, the magnitude of the reciprocal-lattice point represented by the reflection.

In order to increase the speed and accuracy of the energy measurement, it is important to minimize the scan range of the monochromator. For a simple FCC metal, and for reasonable detector solid angles of ~ 0.25 , there should be ~ 1 reflection over a ΔE of ± 100 eV at 20 keV. It should, therefore, be possible to predict the energy of a reflection for a simple FCC metal within ~ 100 eV of a nominal monochromator setting. Experience has shown that monochromator motions on this scale can be reproducibly made within $\sim 0.1-0.25$ eV. A specially monochromator designed and constructed for such measurements will be described in a later publication.

Automatic indexing

As illustrated above, key to measurements with broad-bandpass beams is the ability to index the observed reflections. This important step has been addressed in previous publications^{7,8,9}, but existing methods are often difficult or impossible to use with microdiffraction data on polycrystalline materials; existing methods require many reflections from each grain and are greatly complicated by overlapping patterns. The method described below works well with simple cubic metals where only a few (4-20) reflections are collected for each grain.

The algorithm ORDEX is outlined in the flow chart of Fig. 7. A well calibrated area detector is used to collect overlapping Laue patterns from a polycrystalline sample. The Bragg plane normals and 2θ angles for each reflection are noted and possible indices of each reflection are calculated based on 2θ and the energy bandpass. The angles between the Bragg plane normals of possible

pairs of indices are then compared to find pairs within the estimated measurement and strain uncertainty of the sample. Angles between three and higher numbers of reflections are then compared to identify all reflections from a single grain.

A typical experimental setup to take wide bandpass Laue images is shown in Figure 8. Because synchrotron radiation is polarized in the plane of the storage ring, a CCD above the sample is more efficient than one in the ring plane. The sample can be scanned along 3 orthogonal axes and the CCD can be moved up and down. The vertical detector motion is used to change the angular resolution/solid angle subtended by the detector and to help determine the distance from the detector to the sample.

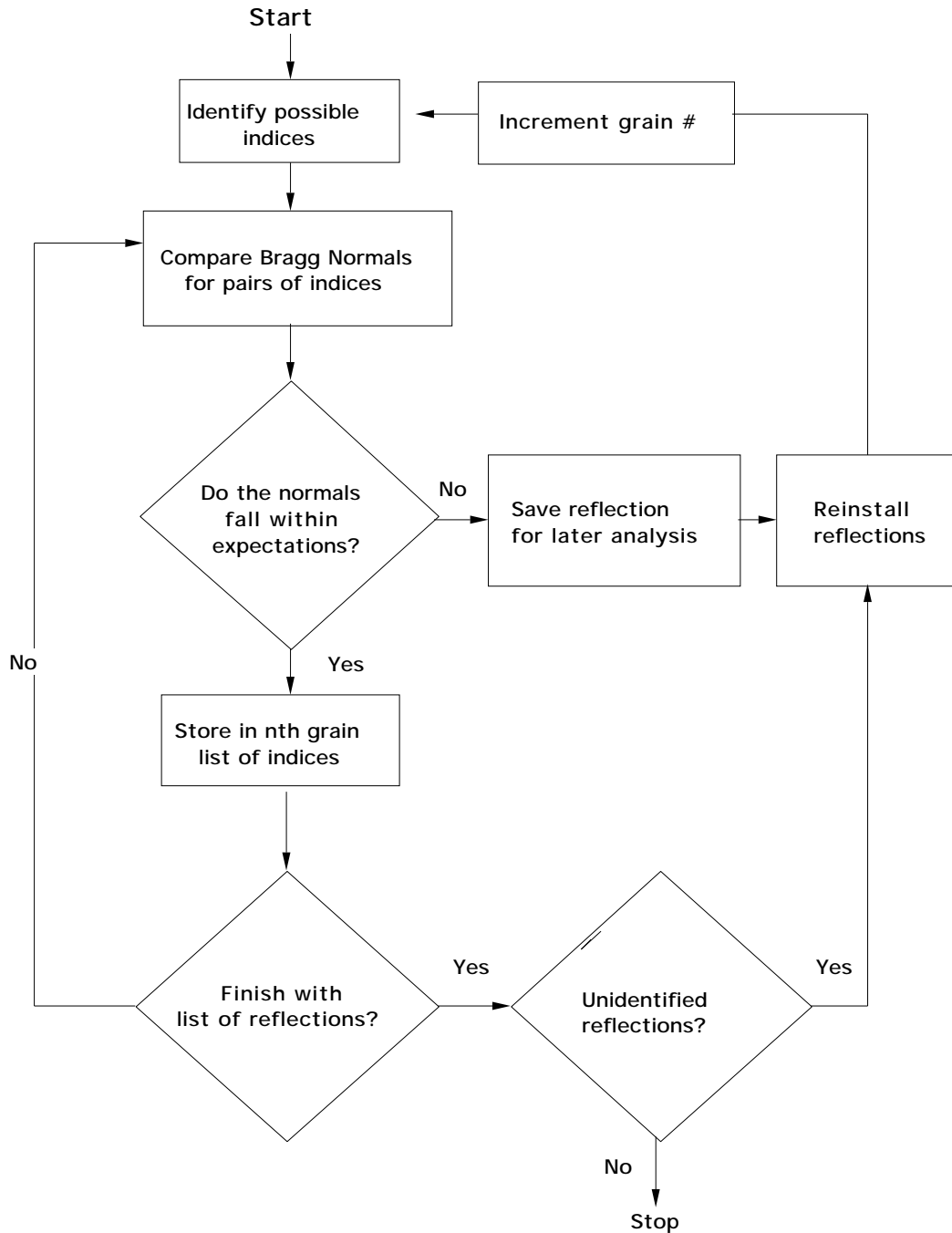


Fig. 7 ORDEX flow chart. The possible indices for each reflection are determined from the known bandpass of the radiation, the known unit cell of an unstrained grain, and the 2θ angle of the reflection. The measured angles between reflections are then compared to the theoretical angles for an unstrained grain with all the possible indices. If the angles lie within the expected experimental and strain uncertainty, then the indices are tentatively assigned to the same grain. If no indices can be found which fall within the expected angular uncertainty, then at least one reflection is stored for later evaluation with a new grain. The flow chart does not show the steps required for calibrating the detector system.

Accurate angle measurements are required for indexing. In general, there are six parameters that describe the position and orientation of the CCD camera relative to the sample-beam intercept. A good estimate of the distance between the sample and the detector can be made by translating the detector and triangulating the relative position of the beam-sample intercept. The measured sample-detector geometry can be further refined by fitting the relative position and angles (pitch, yaw, roll) of the detector to Laue patterns from known single crystals with negligible strain. Additional distortions in the detector introduced by coupling to fiber optics or by deposition of the phosphor screen must also be corrected to obtain high-accuracy angle measurements.

Once the angles of observed reflections are determined, the direction vectors of the reflection normals can be determined (Eq. 11). For a given bandpass and a known crystal structure, there are only a limited number of possible pairs of indices h, k, l 's. The upper bound of h, k , and l is set by the energy bandpass. Also for larger indices, reflections are weaker because atomic scattering factors diminish for large momentum transfer. For indexing purposes, typically indices above 20 can be ignored.

The symmetry of the crystal structure further eliminates certain combinations of indices by selection rules. For any position on the detector, there are only a limited number of possible indices due to the 2-theta angle and the bandpass of the incident x-ray beam. With a reasonable selection of bandpass, a manageable number of possible indices can be obtained. For example, with a 10% bandpass at 20 keV, the number of possible indices for each observed reflection is ~200-500 for a Si crystal. The list of possible indices increases linearly with bandpass which slows the algorithm for very large bandpasses. In ORDEX, a list of possible indices is made for each reflection. The program then compares the measured angles between pairs of reflections to the theoretical angles for an unstrained crystal. It discards pairs if their relative angles do not fall within a selectable angular range of

the theoretical prediction. All possible combinations of indices are checked, until only pairs that are consistent with the known crystal structure are determined. When the relative angles between more than three reflections are checked, the number of possible indices converges quickly.

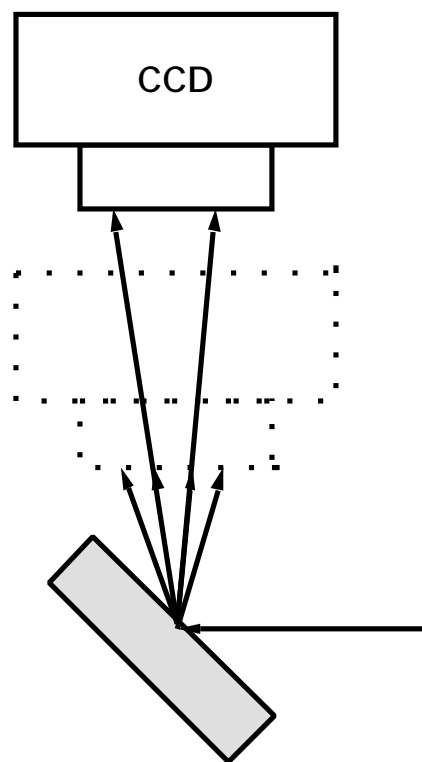


Fig. 8 X-ray microdiffraction geometry showing the area detector positioning for scattering in the vertical plane. This geometry is most efficient for diffraction because the polarization of the incident beam is in the horizontal plane. The detector can be moved (dotted line) to help determine the origin of the diffracted ray.

With more than three non-coplanar reflections, unique pairs can be found by this algorithm. A typical Laue image of Si with an 18-20 keV bandpass and more than 10 reflections takes only a few seconds to index on a Pentium Pro 200 MHz PC. For polycrystalline samples, some reflections

may not have any indices which satisfies the angle requirements because they are from different grains. These reflections are set aside and the program continues to index as many points as possible. Later the algorithm is re-applied to the unindexed reflections to index and identify separate grains. In this way several grains can be indexed from a single Laue image. Even grains of two different crystal structures can be identified. For example, a Laue image from heterostructural thin films can be analyzed to index the reflections from each layer. Once the indices of each layer are determined, the orientation and strain tensors can be found as described previously.

Example

The methods described above are briefly illustrated with a simple example. Two Ge patterns were collected from a monolithic Ge crystal with negligible strain. These patterns were superimposed as shown in Fig. 9 and then the superimposed pattern was automatically indexed to identify the indices of each reflection and to identify which “grain” they belonged to.



Fig. 9 Superimposed images from a Ge single crystal with two independent orientations.

The distortional strain tensor was next calculated from the minimum set of four normal vectors. In this case the vectors used

were the 8 6-6, the 6 6-4, the 3 5 -7, and the 3 3 -3. The distortional strain tensor recovered with this method is,

$$\epsilon_{ij}^{\delta} = \begin{pmatrix} -0.0024 & 0.0000 & 0.0017 \\ 0.0000 & 0.0027 & -0.0011 \\ 0.0017 & -0.0011 & -0.0003 \end{pmatrix}.$$

In this example, the calculated strain tensor indicates the uncertainty of the experimental method. Strain resolution in the plane of the sample is compromised by the limited angular range of the detector and by the limited experimental accuracy of the present CCD system. Much lower distortional strain uncertainties are obtained by fitting to more than four reflections. For example, with the present example, a calculated strain tensor from a non-linear least squares fit to 8 reflections has almost an order of magnitude lower experimental uncertainty;

$$\epsilon_{ij}^{\delta} = \begin{pmatrix} -0.0002 & -0.0002 & 0.0000 \\ -0.0002 & -0.0003 & -0.0002 \\ 0.0000 & -0.0002 & 0.0005 \end{pmatrix}.$$

Although the Ge example may appear to be a particularly simple case, large monolithic single crystals can in fact be a challenge. The intense reflections can cause overflow artifacts in the CCD image and the small divergence of the dynamically diffracted beam means that each reflection illuminates only a few pixels of the CCD. This makes it difficult to accurately locate the center of the reflection. With broader bandpass, more reflections can be collected to further reduce the experimental uncertainty. For example, in cases with 40-60 reflections, uncertainty in the distortional strain tensors of <1 part in 10^4 will be reported in a later paper.

Conclusion

X-ray microbeam allows precision measurements of local strain, stress, and orientation in polycrystalline materials. Overlapping Laue patterns from multiple

grains can be indexed by an iterative process which compares possible indices for several reflections with the observed angles between the reflections. Once the reflections are indexed, the unit cell orientation and unit cell shape can be determined. The volume of the unit cell can be determined with a single energy measurement. The average local strain tensor can be determined from the unit cell parameters.

Acknowledgements

The authors wish to thank Dr. Craig Hartley for a stimulating discussion on the number of reflections required to determine the distortional strain tensor and to Drs. Eliot Specht, Nobumichi Tamura and Bennett Larson for helpful suggestions on the manuscript and on the science of strain mapping in polycrystalline materials. Research sponsored by the Division of Materials Sciences, U.S. Department of Energy under contract DE-AC05-96OR22464 with Lockheed Martin Energy Research. Research in part on MHATT-Cat beamline 7 at the Advanced Photon Source which is funded through the U.S. Department of Energy, Basic Energy Science.

References

1. Buras B. and Tazzari, S. 1984. European Synchrotron Radiation Facility Report of European Synchrotron Radiation Project. Cern LEP Div., Geneva Switzerland.
2. Shenoy, G. K., Viccaro, P. J., and Mills, D. M. 1988. Characteristics of the 7 GeV Advanced Photon Source: A guide for users. ANL-88-9 Argonne National Laboratory, Argonne, IL
3. G. E. Ice, *X-ray Spect.* "Microbeam-Forming Methods for Synchrotron Radiation," **26**, 315-326, (1997).
4. Chevallier, P. and Dhez, P. 1977. Hard X-ray Microbeam: Production and Application. In *Accelerator based atomic physics techniques and applications* (S. M. Shafroth and J. Austin, eds.) pp. 309-348. AIP-Press, New York.
5. Park, Y-H, Yeom, H-Y, Yoon, H-G, and Kim, K-W, "The $\pi/2$ Side-Reflection Laue Technique and the New Chart," *J. Appl. Cryst.* **30**, 456-460 (1997).
6. Patterson, A. L. 1959. In International Tables for X-ray Crystallography, Vol. II, pp. 164-174. Kynoch Press, Birmingham.
7. Sheremetyev, I. A., Turbal, A. V., Litvinov, Y. M., and Mikhailov, M. A., "Computer deciphering of Laue Patterns: application to white synchrotron X-ray topography," *Nucl. Inst. and Meth.* **A308**, 451-455 (1991).
8. Ravelli, R. B. G, Hezemans, A. M. F., Krabbendam, H., and Kroon, J. "Towards Automatic Indexing of the Laue Diffraction Pattern," *J. Appl. Cryst.* **29**, 270-278 (1996).
9. Wenk, H. R., Heidelberg, F., Chateigner, D., and Zontone, F., "Laue Orientation Imaging," *J. Synch. Rad.* **4**, 95-101 (1997).
10. Busing, W. R. and Levy, H. A., "Angle Calculations for 3- and 4-Circle X-ray and Neutron Diffractometers," *Acta Cryst.* **22**, 457-464. (1967).
11. Patterson, A. L. (1959). In *International Tables for X-ray Crystallography*, Vol. II, p. 61, Birmingham: Kynoch Press.
12. Rollett, J. S. (1965). In *Computing Methods in Crystallography*, pp. 22-23, 28-31, Oxford, Pergamon Press.
13. Noyan, I. C. and Cohen, J. B. (1987). In *Residual Stress: Measurement by Diffraction and Interpretation*, p. 33, Springer Verlag, New York.